


## Article

# A Metabolic Control Analysis Approach to Introduce the Study of Systems in Biochemistry: the glycolytic pathway in the red blood cell

Carla R. Angelani  
Pablo Carabias  
Karen M. Cruz  
José M. Delfino  
Marilina de Sautu  
María V. Espelt  
Mariela S. Ferreira-Gomes  
Gabriela E. Gómez\*  
Irene C. Mangialavori\*  
Malena Manzi  
María F. Pignataro  
Nicolás A. Saffioti  
Damiana M. Salvatierra  
Fréchou  
Javier Santos \*  
Pablo J. Schwarzbaum

From the Departamento de Química Biológica and Institute of Biochemistry and Biophysics (IQUIFIB, UBA-CONICET), Facultad de Farmacia y Bioquímica, Universidad de Buenos Aires. Junín 956, C1113AAD, Buenos Aires, Argentina

## Abstract

Metabolic control analysis (MCA) is a promising approach in biochemistry aimed at understanding processes in a quantitative fashion. Here the contribution of enzymes and transporters to the control of a given pathway flux and metabolite concentrations is determined and expressed quantitatively by means of numerical coefficients. Metabolic flux can be influenced by a wide variety of modulators acting on one or more metabolic steps along the pathway. We describe a laboratory exercise to study metabolic regulation of human erythrocytes (RBCs). Within the framework of MCA, students use these cells to determine the sensitivity of the glycolytic flux to two inhibitors (iodoacetic acid: IA, and iodoacetamide: IAA) known to act on the enzyme glyceraldehyde-3-phosphate-dehydrogenase. Glycolytic flux was estimated by determining the concentration of extracellular lactate, the end product of RBC glycolysis. A low-cost

colorimetric assay was implemented, that takes advantage of the straightforward quantification of the absorbance signal from the photographic image of the multi-well plate taken with a standard digital camera. Students estimate flux response coefficients for each inhibitor by fitting an empirical function to the experimental data, followed by analytical derivation of this function. IA and IAA exhibit qualitatively different patterns, which are thoroughly analyzed in terms of the physicochemical properties influencing their action on the target enzyme. IA causes highest glycolytic flux inhibition at lower concentration than IAA. This work illustrates the feasibility of using the MCA approach to study key variables of a simple metabolic system, in the context of an upper level biochemistry course. © 2018 International Union of Biochemistry and Molecular Biology, 00(00):1–14, 2018.

**Abbreviations:** GAPDH; glyceraldehyde-3-phosphate-dehydrogenase;GSH; the reduced form of glutathione;IAA; iodoacetamide;IA; iodoacetic acid; KA; koningic acid;LED; light-emitting diode;MCA; metabolic control analysis;MCTs; mono carboxylate transporter;RBC; red blood cells;TOOS; N-ethyl-N-(2-hydroxy-3-sulfo-propyl)-3-methylaniline;ss; steady state

Volume 00, Number 00, March 2018, Pages 1–14

\*To whom correspondence should be addressed.Tel.: +54 114 964 8289, Fax: +54 114 962 5457.

E-mail: labggomez@gmail.com (G. E. G.), E-mail: irenemangialavori@gmail.com (I. C. M.), E-mail: javiersantosw@gmail.com (J. S.).

Additional Supporting Information may be found in the online version of this article.

All authors contributed equally to this work.

Received 29 March 2018; Accepted 5 June 2018

DOI 10.1002/bmb.21139

Published online 00 Month 2018 in Wiley Online Library  
(wileyonlinelibrary.com)

**Keywords:** Flux control coefficient; lactate flux; response coefficient; glycolysis inhibition

## Introduction

In this article, we describe a teaching module that applies the Metabolic control analysis (MCA) approach to explore the control distribution features of the glycolytic pathway in red blood cells. The first section (*Structure and Activity of Isolated Parts of Metabolic Pathways*) describes aspects of the enzyme GAPDH relevant for this work. The following two sections (*Control Analysis of Metabolic Pathways, Red Blood Cells to Study the Glycolytic Flux and Perturbing the Glycolytic Flux by Adding External Inhibitors*) describe the theory and context introduced by teachers before the lab work is actually performed.

## Structure and Activity of Isolated Parts of Metabolic Pathways

In biochemistry, there are a number of strategies to interrogate a biological system in order to learn about its chemical composition, structure, reactions, molecular mechanisms and function. The classical way to do this is the “*divide and rule*” approach, which laid the foundations of biochemistry and is based on the isolation and purification of individual enzymes and metabolites. Here, one gains interesting information on each one of the constituting parts of the given system.

Before starting this activity, our students are first introduced to the structure and kinetics of key enzymes along this metabolic pathway, and acquire a descriptive knowledge of metabolism. At this stage, students of biochemistry have been trained in the most important features of protein structure and are already familiar with experimental models obtained by X-ray crystallography or NMR, available from the protein data bank (<https://www.rcsb.org/pdb/home/home.do>). Using proper information found in the literature, students are able to localize enzyme active sites, focusing on those amino acid residues important for function. Central to the present work is the glycolytic enzyme GAPDH (PDBID: 4WNC [1], Fig. 1A). This enzyme catalyzes the oxidative phosphorylation of the substrate D-glyceraldehyde 3-phosphate (G3P), which is transformed into the product, 1,3-bisphospho-D-glycerate, a mixed anhydride with high phosphorylation potential, able to synthesize ATP in the next step along this pathway catalyzed by phosphoglycerate kinase. GAPDH includes a typical Rossmann fold as the conserved protein domain whose function is to bind the cofactor NAD. The Rossmann fold typically consists of a six-stranded parallel beta sheet and four associated alpha helices [2].

The thiol group of C152 in GAPDH exerts a nucleophilic addition on the aldehyde group of G3P to yield an enzyme-bound hemithioacetal. Subsequently, the cofactor NAD<sup>+</sup> intervenes to oxidize the adduct (by a usual hydride transfer

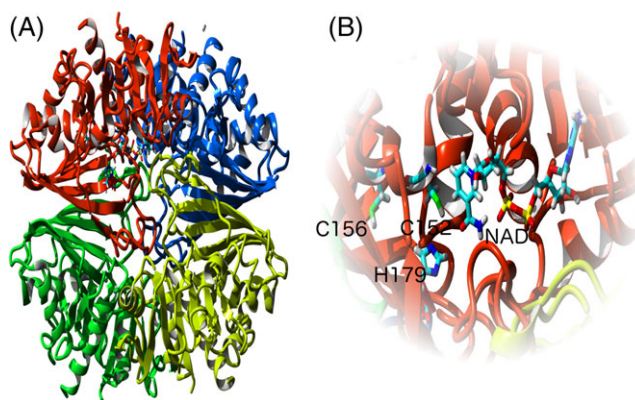


**FIG 1**

The structure of GAPDH. (A) Ribbon model of GAPDH (PDB ID: 4WNC) showing the quaternary structure of the enzyme formed by four subunits (red, blue, green, and yellow). (B) The active site of GAPDH including C152, H179 and the NAD<sup>+</sup> molecule. In addition, residue C156, participating in the reversible oxidation to a disulfide bridge with C152, is also shown. [Color figure can be viewed at [wileyonlinelibrary.com](http://wileyonlinelibrary.com)]

reaction) to a high-energy thioester group, yielding NADH in the process as the by-product. Remarkably, inorganic phosphate exerts phosphorylation of the thioester to yield the high-energy 1,3-bisphospho-D-glycerate product. The side-chain imidazole ring of residue H179 plays a key acid-base role, as it abstracts a proton from the thiol group of C152 at the beginning, donating it back to it at the end of this catalytic cycle [3]. The bound NAD<sup>+</sup> molecule and the key catalytic residues C152 and H179 can be clearly identified in the active site region of the GAPDH structure (Fig. 1B). Moreover, students analyze the chemistry of GAPDH inhibition, that is, they study the irreversible inhibition by each alpha iodo keto reagent: iodoacetic acid (IA) or iodoacetamide (IAA), both reactive with the thiol group of C152, modifying this residue in a covalent form. In addition, they compare the former with the reversible inhibition by oxidation of C152 and C156 to yield a disulfide-linked cystine, a process which occurs inside the cell resulting in protection of C152 against superoxidation [4]. In this case, the enzyme reverts to the active state by reduction of the disulfide bond.

## Control Analysis of Metabolic Pathways

Metabolism as a whole or even single metabolic pathways are complex networks where enzymes and proteins interact through common reactants, substrates, cofactors, and regulators to yield properties which cannot be simply predicted by the kinetics of enzymes in isolation. This is because the interaction between individual parts creates new properties which are inherent to the whole system [5,6].

In this context, MCA provides a suitable system-level framework to study the impact of the parts (individual

metabolic steps) on variables of the system like flux or the concentration of metabolites [7,8]. Metabolic steps are connected mostly by enzymes, but also by transporters. To simplify the treatment, only enzymes will be considered. MCA is applied under steady state conditions [6], characterized by invariant metabolite pools and constant individual net reaction rates that determine constant fluxes ( $J$ ) of metabolites. This methodology has been recently used in important fields, such as cancer therapy [9]; biotechnology, for the redesign of metabolic pathways; [10–12] and the study of the metabolism of parasites [13], pointing out the high relevance of this approach.

A key-concept in MCA is to test the sensitivity of the variables of the system to changes in enzyme, substrate or inhibitor concentrations. Sensitivity is formalized and quantified by coefficients. In particular, the sensitivity of the pathway flux to perturbations on the rate of an individual step  $i$  is characterized by *flux control coefficients* [Eq. 1]:

$$C_i^J = \frac{\partial J_{ss}}{\partial v_i} \cdot \frac{(v_i)_{ss}}{J_{ss}} \quad (1)$$

where  $\partial v_i$  reflects the perturbation on the rate of the reaction catalyzed by the enzyme  $i$  and  $(v_i)_{ss}$  is the rate of this reaction under steady state conditions.  $J_{ss}$  is the metabolic flux of the system under steady state conditions and  $\partial J_{ss}$  reflects the change in flux that results from the rate perturbation  $\partial v_i$ .

Under the MCA formalism, *control* is understood as a property of the whole system and is distributed among all steps of the metabolic pathway [5]. Remarkably, the control achieved by a given enzyme (or transporter) depends on the control exerted by the other enzymes of the pathway, and as Kacser and Burns showed “...questions of flux control cannot be answered by looking at one step in isolation - or even each step in isolation” [6].

Another meaningful tool from MCA that can be applied and that is easy to evaluate in an experimental fashion, is the sensitivity of the systems’ flux to external modulators (such as an enzyme inhibitor). This is formalized by the *response coefficient* [Eq. 2]:

$$R_p^J = \frac{\partial J_{ss}}{\partial p} \cdot \frac{p_{ss}}{J_{ss}} \quad (2)$$

where  $\partial p$  represents a small perturbation in the concentration of the modulator  $p$ , and  $p_{ss}$  is the concentration of this modulator in a given steady state condition.

Interestingly, the concept of response does not involve any assumption on the mechanism of action of the modulator on one or more enzymes, whereas the global flux (or fluxes) is the modulated system variable. In the simple case of a *specific inhibitor*, it will only modify the flux by *the modulation of the rate of the reaction catalyzed by a given*

*enzyme  $i$* , that is,  $v_{iss}$ . This modulation is quantified by the *elasticity coefficient* [Eq. 3]:

$$\varepsilon_p^i = \frac{\partial v_i}{\partial p} \cdot \frac{p}{v_{iss}} \quad (3)$$

Here, a perturbation on the inhibitor concentration  $\partial p$  will result in a variation  $\partial v_i$  of  $v_{iss}$ . It is readily apparent that the variation in  $v_{iss}$  will produce a change in flux according to Eq. 1. In the particular instance of a *specific inhibitor*, an important relationship between elasticity and flux control coefficients can be described by Eq. 4:

$$R_p^J = C_i^J \varepsilon_p^i \quad (4)$$

However, when the inhibitor acts on *more than one metabolic step*, a more general expression is given by Eq. 5:

$$R_p^J = \sum_i C_i^J \varepsilon_p^i \quad (5)$$

Equation 5 is then valid even for nonspecific inhibitors because the overall response coefficient takes into account the sensitivity to the perturbation in the concentration of the modulator  $p$  of each one of the enzymatic activities ( $i$ ) weighted by the control coefficient corresponding to each one of these activities. That is, contributions to the sum only come from the enzymes for which  $\varepsilon_p^i$  is a nonzero value.

Experimental constraints provided by the conventional kinetic approach (coming from the reductionistic “*divide and rule*” view) can enhance the predicting power of mathematical models of the system. In turn, measured experimental sensitivities can be analyzed side-by-side to simulated control coefficients (aided by software such as COPASI, [14]).

We address this practical introduction to MCA based on our teaching experience of several years of imparting this topic within the framework of the course entitled “Advanced Biological Chemistry”, required for every undergraduate student to attain the degree in Biochemistry at the School of Pharmacy and Biochemistry, University of Buenos Aires. MCA represents the subject that most comprehensively encompasses the rest of the issues lectured along the course. To our knowledge, this is the only undergraduate course that imparts this topic in Argentine academic institutions.

### Red Blood Cells to Study the Glycolytic Flux

In humans, circulating red blood cells (RBCs) constitute a heterogeneous cell population exhibiting a life span of approximately 120 days. Amazingly, about  $1 \times 10^{11}$  RBCs are produced daily in the red bone marrow and a similar number is cleared by macrophages [15].

The RBCs is a simple cell model to study metabolism because it lacks organelles, lessening major complexities

due to segregation of enzymes in specific compartments. Besides glycolysis can be studied without significant interference of other metabolic pathways. The RBC glycolytic pathway (Fig. 2A) has been widely characterized [16–18]. Each individual enzyme was isolated, its structure–function–relationships were established and kinetic models were built. Some of these models provide a good match to the *in vivo* metabolic behavior of the cell, mimicking several regulatory features present in glycolysis [19]. Moreover, the effects of mutations and several pharmacological, environmental and hormonal stimuli on RBCs glycolytic flux were well characterized in various physiological and pathological conditions [19–22]. Despite its apparent simplicity, compartmentalization has been well described in RBCs. An outstanding example is GAPDH, which is normally inhibited upon binding to a plasma membrane protein (Band 3), whereas in the presence of deoxyhemoglobin, this enzyme is released into the cytoplasm and becomes active [23]. Thus, the specific activity

of GAPDH depends strongly on the structure and metabolic state of the complete system.

RBCs convert extracellular glucose into intracellular intermediates, along the glycolytic pathway, followed by the transport of the end-product cytosolic lactate to the extracellular medium. The uptake of glucose is facilitated by the GLUT1 transporter [24], whereas lactate is released to the extracellular medium by the monocarboxylate transporter, generically called MCTs [25,26].

In order to convey these notions, prior to the lab work, a simplified, ‘system-oriented’ glycolytic system is introduced to the students (Fig. 2A). Such a metabolic system is thermodynamically open, and can exist in different states. The relevant state for MCA is the so-called steady state or stationary state [6], which requires to maintain constant extracellular glucose and lactate concentrations, constituting the source and sink of the system, respectively. Under these conditions, metabolite pools are time invariant, as are the individual net rates (the velocities of each step), which

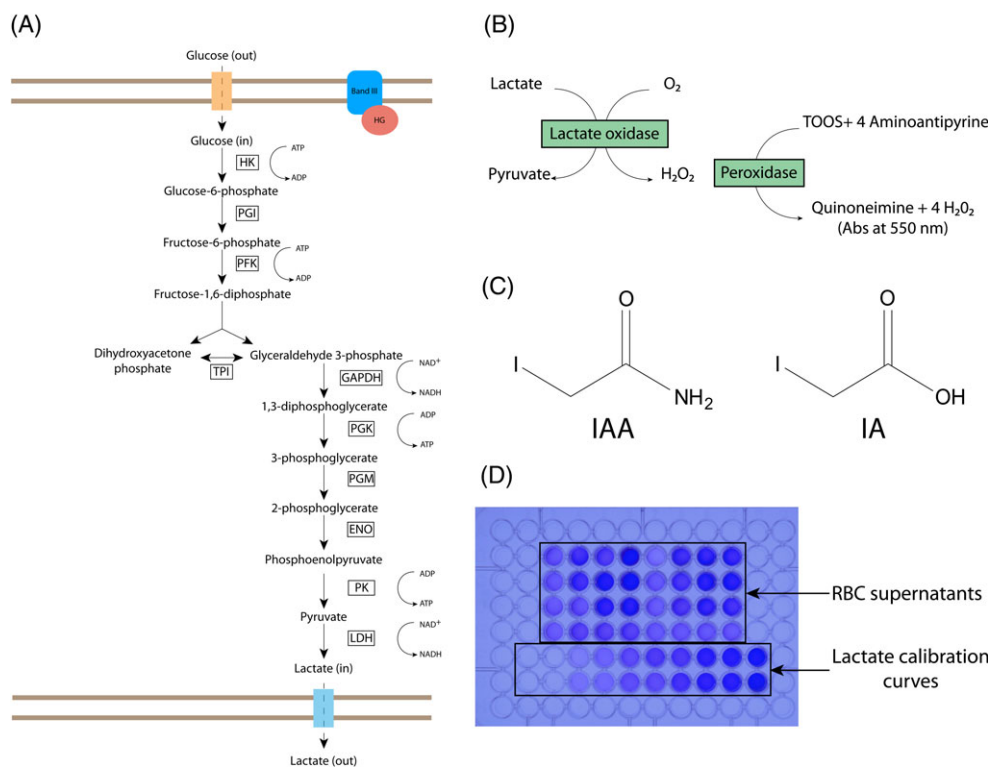


FIG 2

Glycolytic flux in RBC and lactate concentration measurements. (A) The metabolic pathway from extracellular glucose to extracellular lactate. The enzymes involved are the following (in order along the pathway). HK, hexokinase; PGI, phosphoglucose isomerase; PFK, phosphofructokinase I; TPI, triose phosphate isomerase; GAPDH, glyceraldehyde-3-phosphate-dehydrogenase; PGK, phosphoglycerate kinase; AL, aldolase; PGM, phosphoglycerate mutase; ENO, enolase; PK, pyruvate kinase; LDH, lactate dehydrogenase. In addition, Band III and hemoglobin (HG) are also included in the scheme given their importance for the control of the glycolytic flux. The glucose transporter GLUT1 is indicated in orange, and the monocarboxylate transporter (MCT) in light blue. (B) Scheme of the reactions involved in the colorimetric assay for the quantitative determination of lactate. (C) Chemical structures of IAA and IA (D) The image of a 96 well plate showing a typical result of this practice. [Color figure can be viewed at [wileyonlinelibrary.com](http://wileyonlinelibrary.com)]

determine a constant flux (J) of metabolites through the system. Students are guided to recall that in glycolysis metabolites are transformed and transported by specific enzymes or transporters, which in turn display their own-individual-kinetic and structural properties.

In this system, *metabolic concentrations and reaction rates* are the metabolic *variables*, while *parameters* define reaction stoichiometry, enzyme kinetic, and environmental conditions. The magnitudes of these parameters are assumed to remain constant under steady state conditions, except when a controlled perturbation of a single parameter is assayed (parameter scan mode), inducing the system to evolve to a new steady state. As we mentioned in the previous section, a main goal of MCA deals with understanding how a change in the magnitude of a given parameter impacts the variables of the metabolic system.

To carry out the practical work presented here, one needs that extracellular lactate to act as a constant sink, thus assuring the attainment of a steady state. Nevertheless, monitoring the rate of extracellular lactate accumulation is also a methodological requirement to assess the glycolytic flux. [23,27]. To reconcile these apparently contradictory conditions, a minor conceptual trick has to be implemented. In the scheme, we *consider the last reaction as irreversible*, so that extracellular lactate can no longer influence system variables as flux or metabolite concentrations. In this fashion, the concentration of extracellular lactate is then allowed to change (and be experimentally measured as a production rate), knowing that this change is not affecting the system. As a correlate to these considerations, along the experimental leg of this activity irreversible process, that is, it does not affect intracellular lactate or any other system variable, a fact that can be tested experimentally and proved to be true within the boundaries of the conditions assayed. Therefore, small changes in the extracellular lactate concentration are assumed not to affect the thermodynamic strength driving the flux [28]. As we will see below, special care is taken to *wash RBCs with fresh buffer before the experiments*, so that extracellular lactate concentration is kept at a minimum at the start of the experiments. Once the basics of the glycolytic system are all set, we proceed to discuss how to perturb the steady flux by the addition of inhibitors.

### **Perturbing the Glycolytic Flux by Adding External Inhibitors**

IAA and IA (Fig. 2C) are two related inhibitors considered *external* to the glycolytic system, in the sense that their concentrations can be controlled by the experimenter, and therefore can be considered parameters. In principle, these inhibitors act on GAPDH in an irreversible fashion [29], although other effects along the pathway can also be expected. The expected covalent reaction of the alpha halo keto moiety of these reagents is the alkylation of free thiol

groups, yielding stable carbamido methyl (with IAA), or carboxy methyl (with IA) cysteine derivatives. By studying changes in steady flux at different concentrations of these inhibitors, Eq. 2 can be used to derive the corresponding response coefficients that measure the sensitivity of pathway flux. In this manner, the response to IAA, or IA can be compared in a quantitative fashion.

### **Laboratory Course**

In the course 'Advanced Biological Chemistry'-required for all students pursuing the Biochemistry degree at the School of Pharmacy and Biochemistry of the University of Buenos Aires), MCA stands out as a module that comprehensively addresses systemic properties of metabolic pathways.

The laboratory activity described here was thought and designed for advanced undergraduate students of a Biological Chemistry course, focused on intermediate metabolism and its regulation. The activity applies the MCA approach to explore control features of the glycolytic pathway in human RBCs. The MCA module consists of four sessions, of 3 hr each. In Session 1, topic and the underlying theory are introduced; in session 2, a *hands-on* lab work is carried out; in session 3, a computer assisted processing and analysis of the collected experimental data is performed and response coefficients are calculated. Finally, in session 4 students develop a discussion of results and integrate this knowledge with real problems extracted from current scientific articles on this topic.

At the end of the module, each student is required to prepare a final report with the following structure: Introduction, Goals, Material and Methods, Results (presenting data as Figures and Tables), Discussion and Conclusion. It is essential to point out that students will analyze, inform and integrate *the data from all experimental conditions assayed*. Finally, students will discuss the regulatory aspects of the glycolytic pathway within the framework of MCA.

Immediately before starting the laboratory work, instructors wash safety tested deplasmated RBCs by repeated dilution and centrifugation steps to provide the cells with fresh controlled medium consisting of RBC buffer (see *Experimental procedures*) using standard protocols [30]. This procedure approximately 1 hr is a key step to remove any extracellular lactate prior to the experiment. Here, care should be taken to avoid preventable hemolysis.

Students, working in pairs or small groups, start the experiment by adding a known volume of inhibitor solution to the RBC suspension (Supporting Information Table S1) and dividing it into four samples. These are incubated for 0, 30, 60, or 90 min at 37 °C. After that, samples are centrifuged and the supernatants collected to measure extracellular lactate content. Each group of students is assigned two of the eight experimental conditions, for example, group 1 works with conditions A and E (see Supporting Information Table S2). As it is necessary to perform the experiment





in duplicate, each condition is repeated twice by different groups.

Lactate concentration is determined by a colorimetric assay using a commercial kit (*Roche Diagnostics, Indianapolis, Indiana*). A stock solution of lactate is used as reference standard to build a calibration curve in duplicate. Finally, color development is evaluated using a lab-made device useful for extracting absorbance measurements from the 96-well microplate. The acquisition of an *ad hoc* spectrophotometer for microplates becomes the limiting economic factor due to its high cost, especially for laboratories with reduced budgets. The development of an application (the ReadPlate plugin) that fulfills the purpose of analyzing the photographic image of the plate automatically and based on a widely popular, free and open source image processing program (ImageJ: <https://imagej.nih.gov/ij/>) allowed us to respond to the needs of any laboratory. In place of a microplate spectrophotometer, only the following basic equipment is required [31]: (a) a transilluminator (a white LED array covered by an acrylic plate which acts as a light-diffusing base); (b) a regular digital camera (or cell phone camera), and (c) a personal computer where the ImageJ program and the ReadPlate plugin are installed. This application, measures the color intensity of a photographic image of 96-well microplate in any of the three color channels [31]: red, green, or blue (RGB) and returns the blank-corrected absorbance values for each well (for further details refer to the Supporting Information).

### Experimental Procedures

Throughout the laboratory activity, students are divided into eight groups. Each group incubates washed RBCs at two different IAA concentrations for the indicated times. Then, students separate the supernatants by centrifugation and preserve them at room temperature. Once all incubations are finished, samples are charged into a multi-well plate for lactate determination.

### Materials and Reagents for the Laboratory Activity

Materials: Gloves, protection goggles, eppendorf tubes (1.5 mL), capillary tubes, automatic pipettes (200 and 1000  $\mu$ L), pipette tips, incubator at 37 °C, centrifuge for 1.5 mL and 15 mL tubes (room temperature), one personal computer, one cell phone equipped with camera, the ImageJ software and the ReadPlate plugin. Reagents: safety tested fresh deplasmated RBCs, isosmotic RBC medium: buffer (2.7 mM KCl, 137 mM NaCl, 2.5 mM Na<sub>2</sub>HPO<sub>4</sub>, 1.5 mM KH<sub>2</sub>PO<sub>4</sub>, 1 mM MgSO<sub>4</sub>, 1.3 mM CaCl<sub>2</sub>, 20 mM glucose, [30]), distilled water, IAA and IA stock solutions (20, 100 and 500 mM), 6.0 mM sodium lactate solution, lactate detection kit (Roche Diagnostics, Indianapolis, Indiana) including Reagent 1 (3.5 mM N-ethyl-N-(2-hydroxy-3-sulfopropyl)-3-methylaniline (TOOS), ascorbate oxidase (cucumber)  $\geq$  30 U/mL, 100 mM phosphates buffer, pH 7.8, sodium azide <0.1%) and Reagent 2 (5 mM 4-aminoantipyrine;

lactate oxidase  $\geq$ 10 U/mL, horseradish peroxidase  $\geq$ 24 U/mL; 100 mM phosphates buffer, pH 7.8, < 0.1% sodium azide.

### Red Blood Cells Preparation

Adequately safety tested RBCs, stored in citrate / phosphates buffer added with dextrose, are used (RBCs are kindly provided by the Regional Haemotherapy Center Fundosol Foundation). To avoid damage caused by storage, 'fresh' human RBCs are used for all experiments, that is, RBCs from blood drawn within 10 days. The cells are extensively washed at room temperature with isosmotic RBC buffer. Deplasmated RBCs are centrifuged at 500  $\times$  g for 5 min. The supernatant is gently suctioned with a Pasteur pipette and discarded into biohazardous waste. Then, fresh RBC medium is added to the erythrocyte pellet ensuring that the volume of buffer be double that of the pellet. Tubes containing the RBC suspension are capped and inverted a few times to gently mix the content prior to centrifugation at 500  $\times$  g for 5 min at room temperature. The cells are successively washed (seven times) to minimize lactate concentration produced along the storage time. Finally, RBCs are supplemented with sufficient medium to reach a 25% hematocrit. Tubes are frequently mixed by inversion.

### Sample Collection

All steps are carried out at room temperature, except where indicated. Each group of students receives two tubes containing 1.2 mL of RBC suspension (25% hematocrit) in RBC medium (buffer supplemented with 20 mM glucose, see above). To generate the eight different experimental conditions, appropriate aliquots of the IAA (or IA) stock solutions are added and gently mixed. Each tube (two tubes per group) is split into four aliquots, one for each incubation time (0, 30, 60, and 90 min). Immediately thereafter, tubes are centrifuged at 500  $\times$  g for 5 min. The resultant supernatants (60  $\mu$ L) are gently separated, taking care of not perturbing the RBC pellet, and kept until further use. If cells happen to be accidentally re-suspended, a new centrifugation is carried out. At least 20  $\mu$ L of each supernatant is needed for the determination of the lactate content.

### Lactate Measurement

One of the key points of this activity is to rely on an optimized method to measure extracellular lactate. Among techniques commonly applied in clinical chemistry, there are those based on the detection of NADH by its absorbance at 340 nm. This molecule is the product of the oxidation of lactate by the enzyme lactate dehydrogenase (LDH). One main drawback here is the requirement of a UV spectrophotometer. By contrast, other methods are based on the generation of products that absorb in the visible range of the spectrum, therefore making them more suitable for teaching purposes. Among them are methods that employ two coupled reactions catalyzed by the enzymes lactate oxidase (LO) and peroxidase (PO) to generate a product that

absorbs at 555 nm. This latter approach combined with the low volume requirement of the ReadPlate system allowed us to carry out this activity at a lower cost than classic colorimetric determinations with a conventional spectrophotometer.

In our proposed activity, lactate concentration is determined by an enzymatic assay, which ultimately results in a chromogenic product that can be quantified at 555 nm, and that is proportional to the lactate present in the sample. The typical detection range for this kit is between 0.2 and 10 nmol of lactate. Most conveniently, there is no need for pretreatment or purification of samples, and usually hemolysis is so low that it does not interfere with color determination. Typically, a volume of 20  $\mu\text{L}$  of either sample or calibration solution (final lactate mass: 0–40 nmol) is placed in a 96 multi-well plate and 90  $\mu\text{L}$  of Reagent 1 is added. After incubation for 2 min at 37  $^{\circ}\text{C}$ , the multi-well plate is placed on top the transilluminator (Supporting Information Fig. S2) and a snapshot for blank control is taken. Then, Reagent 2 (18  $\mu\text{L}$ ) is added to each well and the plate is incubated at 37  $^{\circ}\text{C}$  for 15 min. At the end, a second snapshot is taken. These pictures are then subjected to color intensity analysis (Supporting Information Figs. S1,S2, followed by quantification with the custom-built ReadPlate plugin (<https://imagej.nih.gov/ij/plugins/readplate/index.html>, instructions for use embedded), written for the free ImageJ software. Importantly, to validate the technique, parallel measurements were carried out using a standard commercially available multi-mode microplate absorbance reader (BioTek Instruments Inc. Winooski, Vermont, USA). The correlation plot between absorbance readings estimated with each device is shown in Supporting Information Fig. S3. It should be emphasized that control samples were included to demonstrate that the inhibitors assayed do not interfere with the reaction for lactate detection.

### System Response Calculation

To determine the response of the flux of the system to the added inhibitor, we empirically found appropriate to fit a ratio of polynomials to the flux data ( $J_{ss}$ ). Thus, Eq. 6 provides a reasonable fit to the behavior of flux as a function of the inhibitor concentration assayed, with a minimal number of parameters:

$$J_{ss} = \frac{(a_0 + a_1[inh] + a_2[inh]^4)}{(1 + b_1[inh] + b_2[inh]^4)} \quad (6)$$

Here,  $a_0$ ,  $a_1$ ,  $a_2$ ,  $b_1$  and  $b_2$  represent the fitting parameters, and  $[inh]$  is the inhibitor concentration. In

particular, one should notice that in the absence of inhibitor, the flux equals  $a_0$ . In addition, the derivative of this function can be easily calculated analytically [students should realize that they can use simple rules, like the quotient or the chain rule, to calculate Eq. 7]:

If  $\frac{\partial J_{ss}}{\partial [inh]}$  is multiplied by the corresponding value of  $[inh]$  and divided by the corresponding flux value  $J_{ss}$  of the system at that particular inhibitor concentration, we obtain the expression for the *response coefficient* [Eq. 8]:

$$R_{inh}^J = \left( \frac{\partial J_{ss}}{\partial [inh]} \right) \frac{[inh]}{J_{ss}} \quad (8)$$

that is similar to Eq. 2. This may be done using an Excel spreadsheet, such as the one provided as a Supplementary Material file of this article. Alternatively, after fitting Eq. 6 to the flux data, the response coefficient at any given inhibitor concentration can also be obtained analytically [Eq. 9]:

$$R_{inh}^J = \frac{(a_1[inh] + 4a_2[inh]^4)}{(a_0 + a_1[inh] + a_2[inh]^4)} - \frac{(b_1[inh] + 4b_2[inh]^4)}{(1 + b_1[inh] + b_2[inh]^4)} \quad (9)$$

Here, students should notice that  $R_{inh}^J$  becomes null in the absence of inhibitor.

## Results

### Lactate Calibration Curves

One of the most relevant features of the MCA approach is the possibility to describe the response of the system and the distribution of control along the metabolic pathway in a quantitative fashion. In the case under study, the accurate quantification of end-product lactate is an important issue for the correct determination of the glycolytic flux (Fig. 2A).

To quantify lactate, of central importance is to calibrate the assay by taking into account a reference curve with known lactate masses. Fig. 2B shows a scheme of the coupled reactions that easily allow the student to carry out lactate measurements. On the other hand, Fig. 2D shows a snapshot of a 96-well plate representative of the results typically obtained when the colorimetric reaction is completed. The calibration curve (run by duplicate) is independently obtained by different groups of students: absorbance values are plotted as a function of lactate mass (Fig. 3A and Table I). It is noteworthy that linearity is observed up to 40 nmol of lactate, a useful upper limit for the ensuing measurements.

---


$$\frac{\partial J_{ss}}{\partial [inh]} = \frac{(a_1 + 4a_2[inh]^3)(1 + b_1[inh] + b_2[inh]^4) - (a_0 + a_1[inh] + a_2[inh]^4)(b_1 + 4b_2[inh]^3)}{(1 + b_1[inh] + b_2[inh]^4)^2} \quad (7)$$


---

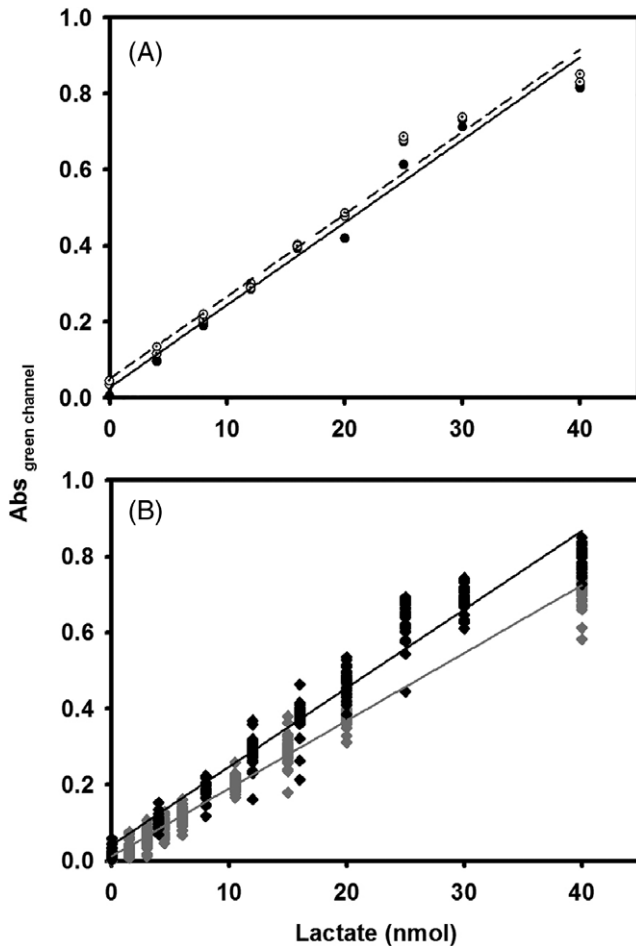


**FIG 3**

Lactate calibration curves. Color intensity in each well is integrated and absorbance values calculated by ReadPlate from snapshots of 96-well plates (see Supporting Information) where the assay is run for the colorimetric detection of lactate. Dilutions of standard lactic acid solutions (20, 100, and 500 mM) are used. (A) Values obtained by a group of 20 students for a given plate (black circles) or for its duplicate (open circles). (B) Calibration curves obtained by students who completed the course in 2016 (gray diamonds) or in 2017 (black diamonds). Straight lines obtained after linear regression are also shown in each case.

We also tested the performance of lactate detection after dilution of reagents up to 10 times, noting that the assay remains functional, but the linear range becomes shorter at higher dilutions. Therefore, to reduce costs without compromising the performance, we decided to dilute reagents only to one half. This dilution represents a good choice, because it guarantees a uniformly linear response in the green channel. Fig. 3B and Table I shows results obtained by groups of students along two consecutive periods of classes (2016 and 2017). High reproducibility is observed by comparison of the results of these two cohorts.

**TABLE I**

Calibration curves for lactate

	Slope ( $Abs \times nmol^{-1}$ )	
One group of students (2017)	$0.0217 \pm 0.0009$	$0.0216 \pm 0.0009$
2016 cohort		$0.0178 \pm 0.0001$
2017 cohort		$0.0208 \pm 0.0003$

Solutions of different concentrations of lactate were used to build a calibration curve using reagents from the kit Roche Diagnostics (Indianapolis, Indiana) and photographs of 96-well plates (Supporting Information Fig. S3). As an example, this table shows the slopes of the calibration curves obtained by one group of 20 students (2017) for one plate measured in duplicate. Likewise, the averages of the slopes measured by all groups of students who completed the course in 2016 (cohort 2016) or in 2017 are shown. The standard deviations of each result are also indicated.

### Glycolytic Flux Measurements and its Inhibition by IAA

As indicated above, we measure the glycolytic flux in the presence of different IAA concentrations by quantifying the amount of extracellular lactate secreted by RBCs as a function of incubation time (Fig. 4). RBCs storage under blood bank conditions produces significant biochemical alterations [15], in particular after the first 2 weeks of storage [32]. Quantitative differences in the glycolytic flux and regulation features of this metabolic pathway may be observed, depending on the aging *in vitro* of the cells, thus becoming of the utmost importance to work with freshly drawn RBCs.

Results from a typical experiment carried out in duplicate by one group of students are shown in panels A and B of Fig. 4. To estimate values for the flux, students process data by linear regression on each time series corresponding to a given inhibitor concentration assayed. Results are shown as a combined plot including all available data. As expected, in the absence of IAA, the lactate amount in the supernatant shows the largest increment with time, thus demonstrating that RBCs remain metabolically active under these experimental conditions: 90-min incubation at 37 °C in RBC buffer, 20 mM glucose. Importantly, no significant hemolysis is observed along this incubation period, values of lactate concentration at the start of the experiment are very similar for all conditions tried, and the colorimetric reaction for lactate assay does not suffer interference by the inhibitor up to the highest concentration assayed. Most significantly, the linear production of lactate observed as function of time is consistent with the main condition necessary to apply this kind of analysis, that is, that the system should comply with the steady state.



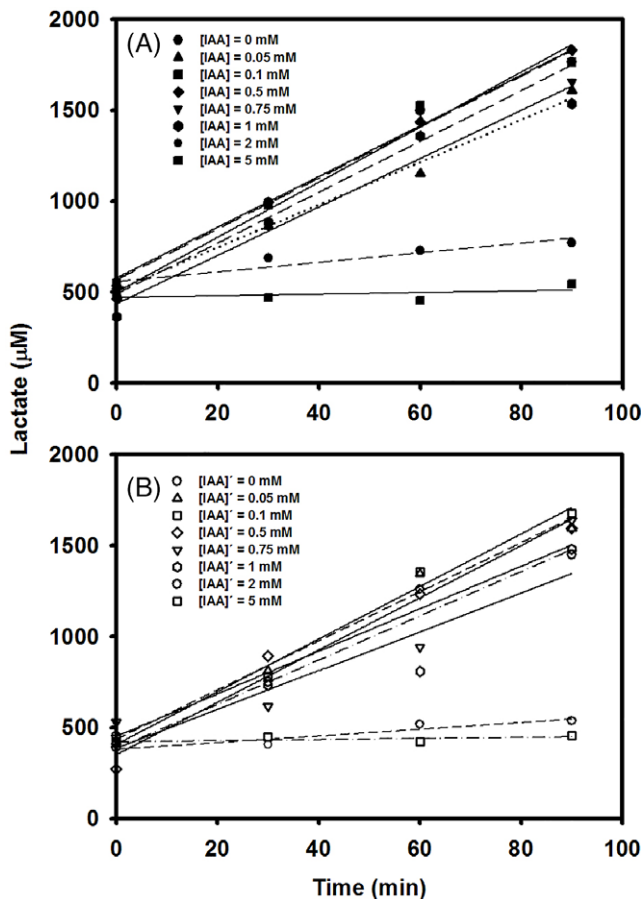


FIG 4

Lactate production rate for different inhibitor concentrations. Concentration of extracellular lactate produced by red blood cells is determined at four incubation times (0, 30, 60, and 90 min) using the Roche diagnostic kit (Experimental Procedures). Results obtained for each concentration of IAA by one group of 20 students are shown in (A). Duplicates of each one of the measurements are shown in (B).

On the other hand, the presence of the IAA inhibitor decreases the production of lactate, particularly when cells are exposed to an IAA concentration higher than 1 mM. In fact, exposure to 5 mM IAA results in a complete abrogation of lactate production. By this time of the activity, students realize that IAA causes a major disruption of the metabolic pathway involved in lactate generation: glycolysis coupled to lactate fermentation.

Remarkably, each inhibitor concentration determines a different steady state, characterized by a particular lactate flux. Through simple inspection, students can easily compare the measured fluxes. In addition, calculation of the standard error associated to the linear regression fit allows one to evaluate the accuracy of lactate flux measurements. Our collected experience points to the overall robustness of the resulting dataset.

Results of flux ( $J_{IAA}$ ) data as a function of IAA concentration obtained by two independent groups of students of the 2017 cohort is plotted in Fig. 5A and Table II. The profile of flux variation with IAA incremental concentration is very reproducible. Accumulated data obtained by all student groups during 2016 and 2017 are plotted together (Fig. 5B and Table II). Some interesting points for discussion arise from the observation of the shape of the graph. First, different regions can be clearly defined in the  $J_{IAA}$  versus  $[IAA]$  curves. Actually, a slight *increment in flux* (more evident in the 2017 dataset) can be observed at low IAA concentration. On the other hand, at concentrations higher than 0.5 mM, IAA brings about a clear inhibition of the pathway flux. The flux decreases abruptly at concentrations of IAA between 1 and 2 mM, reaching almost null values at approximately 5 mM.

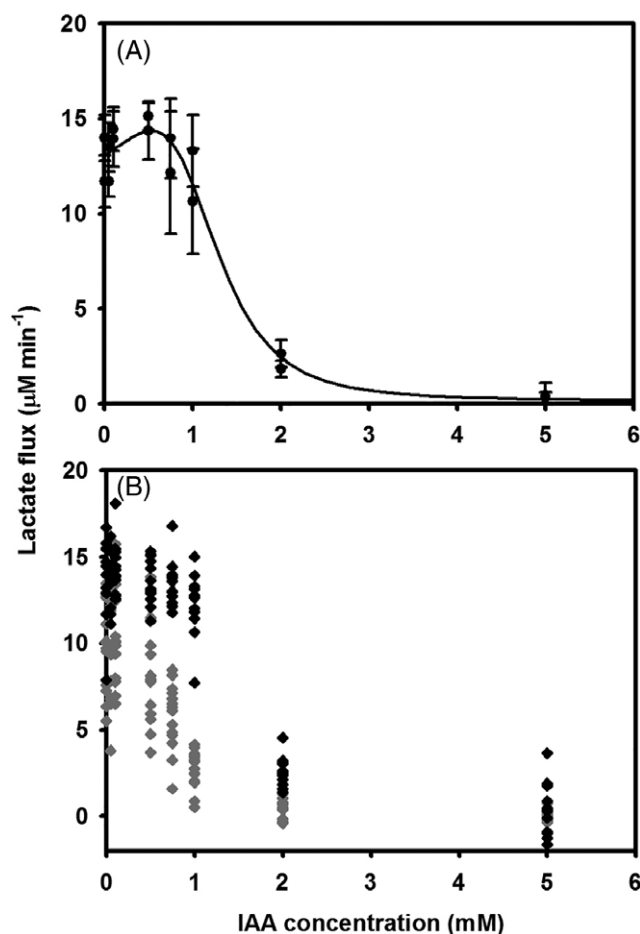


FIG 5

Flux of lactate produced by RBCs incubated at different IAA concentration. (A) Flux data calculated from the slope of the straight lines in Fig. 4. The standard deviation of the measurements is indicated by the error bars. (B) The averages of those fluxes determined by all groups of students who completed this practice in 2016 and 2017.

**TABLE II**
**Glycolytic fluxes evaluated as lactate production measured at different inhibitor concentrations**

IAA (mM)	Glycolytic flux ( $\mu\text{M min}^{-1}$ )			
	One group of students (2017)		2016 cohort	2017 cohort
0.00	$14.0 \pm 1.2^a$	$11.7 \pm 1.4^b$	$10.6 \pm 3.0$	$13.6 \pm 2.3$
0.05	$11.7 \pm 0.8$	$13.5 \pm 1.3$	$10.4 \pm 3.4$	$14.1 \pm 1.6$
0.10	$13.9 \pm 1.4$	$14.5 \pm 1.2$	$10.4 \pm 2.7$	$14.5 \pm 1.5$
0.50	$15.1 \pm 0.7$	$14.4 \pm 1.5$	$8.8 \pm 3.3$	$13.6 \pm 1.3$
0.75	$14.0 \pm 2.1$	$12.2 \pm 3.2$	$5.8 \pm 1.9$	$13.6 \pm 1.3$
1.00	$13.3 \pm 1.9$	$10.6 \pm 2.8$	$2.7 \pm 1.1$	$12.2 \pm 1.7$
2.00	$2.6 \pm 0.7$	$1.8 \pm 0.4$	$0.4 \pm 0.6$	$2.7 \pm 0.9$
5.00	$0.4 \pm 0.7$	$0.3 \pm 0.3$	$0.0 \pm 0.4$	$0.4 \pm 1.4$

Glycolytic fluxes measured as lactate production were calculated from the slopes of the straight lines shown in Fig. 2. This table shows those flows calculated by one group of 20 students for <sup>a</sup>one microplate, and <sup>b</sup>for its duplicate. In addition, the averages of fluxes calculated for each IAA concentration by all groups of students who completed the course in 2016 or 2017 are shown. The standard deviations of each result are also indicated.

### System Response to the GAPDH Inhibitor IAA

Further analysis was carried out to address the issue of the sensitivity of flux to the presence of inhibitors. Fig. 6 shows the fitting of Eq. 6 to the glycolytic flux data and the behavior of the calculated flux response to IAA concentration ( $R_{IAA}^J$ ). This exercise in nonlinear regression allows one to recover, in a simple way, the derivative function  $\frac{\partial J_{ss}}{\partial [IAA]}$  [Eq. 7] and the response coefficient  $R_{IAA}^J$  [Eq. 8]. After the initial fit, the latter can be more straightforwardly calculated with Eq. 9.

Here again, three different regions can be observed in the  $R_{IAA}^J$  curve. The first one (in the range of IAA concentrations between 0 and 1 mM) is characterized by slightly positive values of the response coefficient. In the second region (the range between 1 and 2 mM) highly negative values of the coefficient are observed, indicating that the glycolytic flux becomes highly sensitive to a change in the inhibitor concentration. This region highlights the fact that subtle changes in the inhibitor concentration can produce a large change in glycolytic flux. In other words, under this metabolic condition, for example, the steady-state flux measured at 1.5 mM IAA, the glycolytic flux exhibits high sensitivity to inhibition, presumably due to a small change in GAPDH activity. The third region (IAA concentrations higher than 2.2 mM) is dominated by very low glycolytic fluxes, and

response coefficients approach zero at IAA concentrations higher than 3 mM.

The variation observed in glycolytic flux may be mainly attributed to an effect of the inhibitor targeting GAPDH activity. However, in the cell it has been reported that IAA reacts with the reduced form of glutathione (GSH) as well, hence affecting the redox potential of the cytoplasmic compartment and compromising the GSH metabolism [29]. In this complex context, IAA cannot be considered a specific enzyme inhibitor, thus precluding the calculation the flux control coefficient of GAPDH ( $C_{GAPDH}^J$ ) on the glycolytic pathway by merely taking into consideration the response flux coefficient ( $R_{IAA}^J$ ) and the elasticity value of GAPDH by IAA ( $\epsilon_{IAA}^{GAPDH}$ ), as in Eq. 5.

### Different Responses to IA and IAA inhibitors

We also analyze the effect of IA as a potential inhibitor of the glycolysis and lactate fermentation pathway (Fig. 7). It has been reported that IA behaves as a more potent inhibitor for GAPDH because it interacts more favorably with this enzyme than IAA [29]. In Fig. 7, glycolytic flux as a function of IAA or IAA concentrations is plotted side by side for comparison. Strikingly, the maximal effect of IA is observed at very low inhibitor concentration (about 0.1 mM), well below that where IAA shows its top effect (2.2 mM: more than 20 times higher than the former). Although similar in regard to their chemical reactivity, the response to each inhibitor is completely different. These results agree well with those observed in other cell types like astrocytes, that showed the differential effect of these inhibitors on the cell thiol-disulfide-based redox system [29]. IAA can compromise the cellular glutathione metabolism much more severely than IA [29]. For this reason, it is likely that the effective concentration of IA inside the RBCs be higher than that reached by IAA because the latter reacts in a higher extent than the former with the thiol group from reduced glutathione. On the other hand, IA and IAA might differ at the level of their action on the transport of lactic acid. One can speculate that the enhanced IA effect might profit from co-opting the anion transport machinery (the MCT, Fig. 2), facilitating its entry to the cytosolic compartment and/or altering the outward flux of lactic acid. Although we found no specific reports about this point, it may be an interesting issue for discussion with the students in class. Interestingly, for IAA it was found the steady state with the highest response coefficient reaching the value  $R_{IAA}^J \sim -3.0$ , whereas for IA the coefficient takes a value of  $R_{IA}^J \sim -2.3$ .

As it was mentioned before, it would be useful to take advantage of the response coefficient to evaluate the flux control coefficient of GAPDH. However, to carry out this analysis in the most straightforward fashion, it is necessary that the modulation of the glycolytic flux be caused by a *specific inhibitor* of the enzyme [thus enabling the valid application of Eqs. 4, 5], because, only in this case, the change

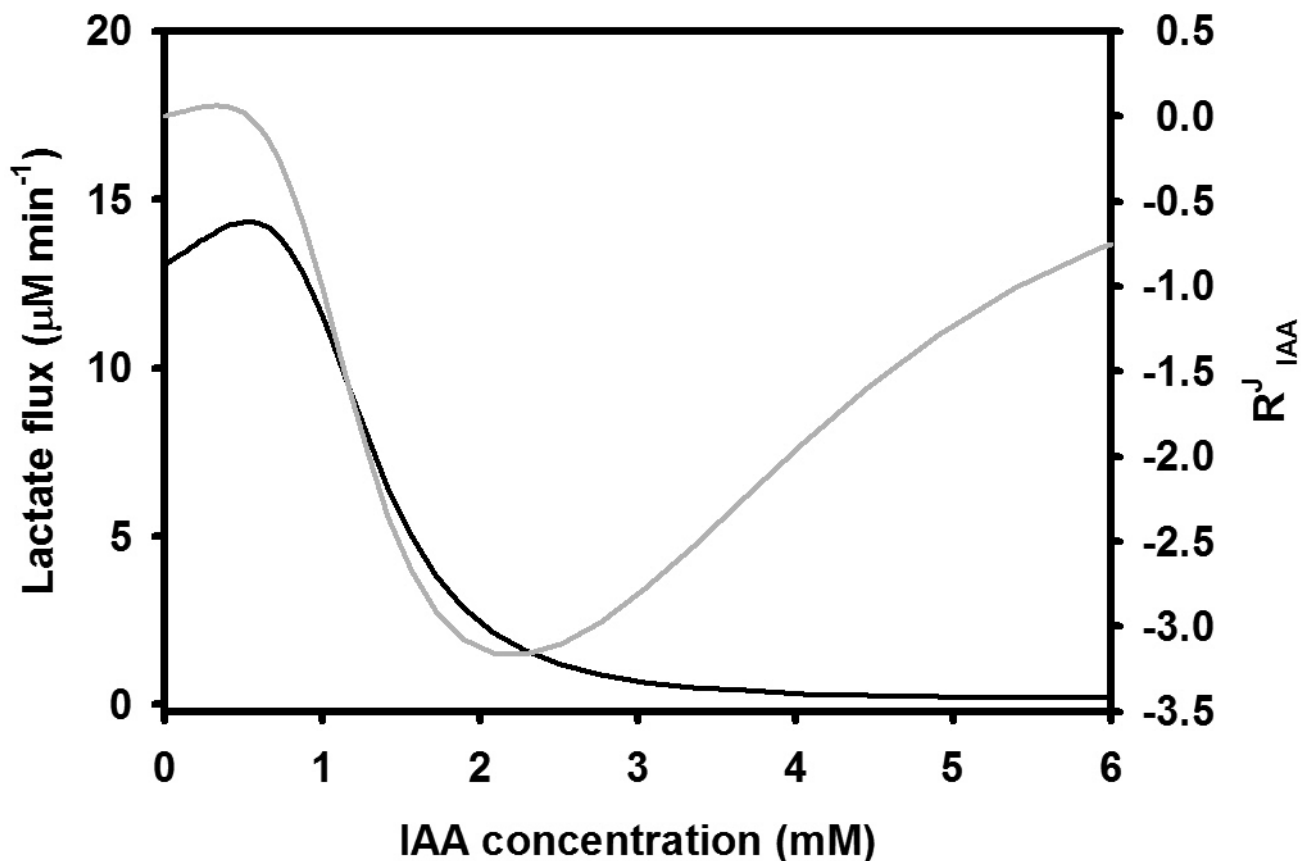


**FIG 6**

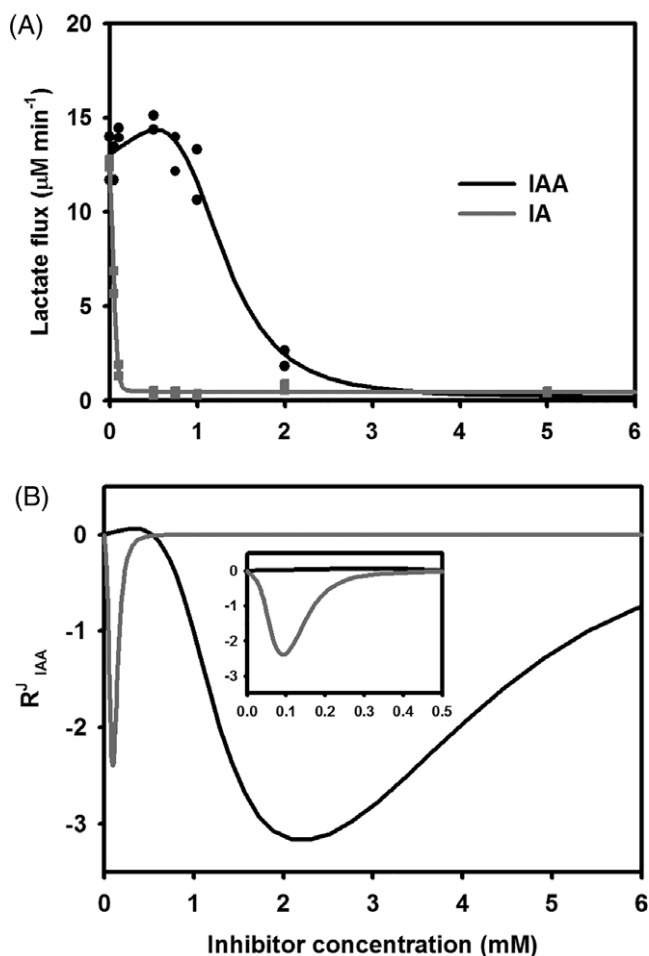
*Sensitivity of lactate flux in RBCs to the IAA inhibitor. The behavior of the flux response coefficient to [IAA] [defined by Eqs. 7, 8, or Eq. 9] is shown in gray line. The same fitted curve as in Fig. 5A is shown in black line as a reference.*

produced in flux would be entirely triggered by the change in the activity of a single enzyme (numerically described by the *elasticity* of this enzyme to the inhibitor). Only in this fashion Eq. 4 might be applied to calculate the control coefficient of this enzyme. In this regard, it will be extremely interesting to study the behavior of the irreversible inhibitor koningic acid (KA), a natural product, which was found to be a selective inhibitor of GAPDH [33–35]. The elasticity coefficient of GAPDH from RBCs for KA can be experimentally calculated. In the end, the use of Eq. 4 would enable us to infer whether GAPDH behaves indeed as a flux-controlling enzyme of glycolysis and more importantly, in which magnitude the enzyme exerts this control.

### Perspectives

In the last three decades MCA has been extended to deal with basically all types of metabolic structures, including enzyme–enzyme interactions and channeling [36] and complex physiological processes such as excitation-contraction and mitochondrial energetics in myocytes [37]. Teachers should assess how much detail of the theory should be included in an undergraduate Biochemistry level, depending on the academic context.

The approach outlined here introduces the student to a simple laboratory work, with focus on the concept of pathway flux, studied as a system variable, and the consequences of altering this flux by changing a parameter of the system, in this case, the concentration of an external inhibitor. A key conceptual aspect is that the inhibitor acts locally on one or more enzymes, but the perturbation is transmitted to the network ultimately affecting the flux, the magnitude of which being quantified by the response coefficient [Eq. 8]. The activity, as such, is closely guided, in the sense that the protocol and the experimental design are already set in advance. Upon this basis, it is anticipated that in future activities students will be given the opportunity to design and plan an experiment of their own to test the sensitivity of pathway variables. This effort should be complemented with mathematical modeling of the system, which is an essential tool to raise hypotheses in advance and make the most of the analysis of the acquired experimental data afterwards. In addition, the sensitivity of pathway variables can be studied in connection with their relevance in medical and biotechnological contexts. A few hints are given below.


**FIG 7**

Comparison of IAA and IA as modulators of the glycolytic flux in RBCs. (A) Lactate flux from RBCs as a function of IAA (black circles) or IA (gray squares) concentration. Each flux value is calculated from the slope of the straight-line kinetics measured at each steady-state condition. Continuous traces correspond to the nonlinear best fit to the experimental data of the function described by Eq. 6. (B) Sensitivity of lactate flux from RBCs to the inhibitor IAA (black line) or IA (gray line), as illustrated by the response coefficient dependence with inhibitor concentration. The inset shows the behavior of the response coefficient in a range of low inhibitor concentration.

#### • Medical Examples

Medical applications of the approach include identifying enzymes/transporters as suitable targets for cancer therapy [38]. To date this task has proved difficult, mainly because of the interlinking of disease pathways through the metabolic network. It is in this context that the MCA framework could help identify target sites for tumor growth that have maximal impact on the metabolic pathway flux and then direct drug development to assure maximal drug action

[39]. In the same fashion, the MCA framework is being applied to provide rational and quantitative criteria to choose the target enzymes for drug development [40].

#### • Biotechnological Examples

Although MCA still remains little known by biotechnologists, it may well provide the key to understanding why the impact of genetic manipulation on the production of commercial metabolites has been rather disappointing [8,41]. In this respect, students could make use of curated mathematical models of yeast glycolysis of various degrees of complexity, which contain the complete set of equations describing the velocities of each metabolic step. These models may be then loaded into modeling programs such as COPASI [14], so as to simulate the dynamic changes of system variables when the magnitude of system parameters is altered. This approach could be used to identify key targets that allow increasing the production of biotechnologically relevant products, such as ethanol [11] or glycerol [42], and analyze the suitability of already available yeast strains. It may also be an opportunity to compare the sensitivity of glycolysis in yeast, as opposed to that observed in RBCs.

#### Limitations in Application of the MCA Approach

MCA has been commonly used to describe how changes in enzyme activities of a given metabolic pathway determine the form in which metabolic variables (fluxes and metabolite concentrations) respond. This is defined by means of the response and control coefficients. However, the strategy was originally developed to predict the effect on system variables of *infinitesimal changes* in activities [a  $\delta v_i$  gives rise to a  $\delta J_{ss}$ , Eq. 1]. In some cases, the inability of increasing a given flux by changing the activity of a particular enzyme is due to an unexpected decrease of the control coefficient of this enzyme when its activity has been increased. Remarkably, other approaches were also developed, which consider coefficients for *large changes*. Indeed, here quantitative and qualitative differences were found in the response by comparison with *the infinitesimal* treatment [43,44]. This should be taken into account in metabolic pathway engineering when larger responses are required, for example, in the case of biotechnological applications.

## Conclusions

This laboratory activity has been successfully implemented along two yearly editions of an undergraduate course of advanced biological chemistry. This course is currently imparted on the third year of the curriculum of the Biochemistry career at the School of Pharmacy and Biochemistry at the University of Buenos Aires. Students found no difficulty in fulfilling the wet-lab segment of this activity because it does not require complex laboratory skills. However, they struggle with data processing because of the mathematical skills required to calculate the coefficients,

which they find more difficult than expected. In particular, the use of tools like nonlinear optimization with Solver, as implemented in Excel, and general abilities for data management in this spreadsheet result new for approximately 70% of the students. Therefore, our cumulative experience suggests that, before actually tackling this MCA practical exercise, students should be encouraged to gain some training in the use of these all too important tools. In addition, key regulatory features of the glycolytic pathway should be introduced in advance, specifically those aspects relevant for the case of RBCs. In this fashion, students will be benefited the most to grasp the nuances of the MCA approach, thus putting them in a position to gain for the first time, individual experience with quantitative system-level methodologies useful for metabolic studies.

## Acknowledgement

This work was supported by grants, facilities and materials provided by the Department of Biological Chemistry, School of Pharmacy and Biochemistry, University of Buenos Aires (FFyB-UBA), and by the National Research Council (CONICET). We expressly thank the Regional Haemotherapy Center Fundosol Foundation for providing safety tested human RBCs samples. We also thank Juan Pablo Rossi and Jeremías Incicco for sharing expertise in handling RBCs and help with the kinetic analyses, respectively. Finally, we specially thank the biochemistry student cohorts 2015–2017 at FFyB-UBA for their contribution and feedback with this laboratory practice.

## REFERENCES

- [1] White, M. R., Khan, M. M., Deredge, D., Ross, C. R., Quintyn, R., Zucconi, B. E., Wysocki, V. H., Wintode, P. L., Wilson, G. M., Garcin, E. D. (2015) A dimer interface mutation in glyceraldehyde-3-phosphate dehydrogenase regulates its binding to AU-rich RNA. *J. Biol. Chem.* 290, 1770–1785.
- [2] A.L. Lehninger, D.L. Nelson, M.M. Cox (2013) Principles of biochemistry, 6th. ed., W.H. Freeman, New York.
- [3] J. McMurry, T.P. Begley (2005) The organic chemistry of biological pathways, Roberts and Co Publishers, Englewood, CO.
- [4] Rinalducci, S., Marrocco, C., Zolla, L. (2015) Thiol-based regulation of glyceraldehyde-3-phosphate dehydrogenase in blood bank-stored red blood cells: A strategy to counteract oxidative stress. *Transfusion* 55, 499–506.
- [5] D. Fell (2007) Understanding the control of metabolism, Portland Press, London.
- [6] Kacser, H., Burns, J. A. (1973) The control of flux. *Symp. Soc. Exp. Biol.* 27, 65–104.
- [7] Fell, D. A. (1992) Metabolic control analysis: A survey of its theoretical and experimental development. *Biochem. J.* 286(Pt 2), 313–330.
- [8] Moreno-Sanchez, R., Saavedra, E., Rodriguez-Enriquez, S., Olin-Sandoval, V. (2008) Metabolic control analysis: A tool for designing strategies to manipulate metabolic pathways. *J Biomed Biotechnol* 2008, 597913.
- [9] Liberti, M. V., Dai, Z., Wardell, S. E., Baccile, J. A., Liu, X., Gao, X., Baldi, R., Mehrmohamadi, M., Johnson, M. O., Madhukar, N. S., Shestov, A. A., Chio, I. I. C., Elemento, O., Rathmell, J. C., Schroeder, F. C., McDonnell, D. P., Locasale, J. W. (2017) A predictive model for selective targeting of the warburg effect through GAPDH inhibition with a natural product. *Cell Metab.* 26(648–659), e648.
- [10] Zhang, Y., Meng, Q., Ma, H., Liu, Y., Cao, G., Zhang, X., Zheng, P., Sun, J., Zhang, D., Jiang, W., Ma, Y. (2015) Determination of key enzymes for threonine synthesis through in vitro metabolic pathway analysis. *Microb. Cell Factories* 14, 86.
- [11] Cintolesi, A., Clomburg, J. M., Rigou, V., Zygourakis, K., Gonzalez, R. (2012) Quantitative analysis of the fermentative metabolism of glycerol in *Escherichia coli*. *Biotechnol. Bioeng.* 109, 187–198.
- [12] Angermayr, S. A., Hellingwerf, K. J. (2013) On the use of metabolic control analysis in the optimization of cyanobacterial biosolar cell factories. *J. Phys. Chem. B* 117, 11169–11175.
- [13] Pineda, E., Encalada, R., Vazquez, C., Nequiz, M., Olivos-Garcia, A., Moreno-Sanchez, R., Saavedra, E. (2015) In vivo identification of the steps that control energy metabolism and survival of *Entamoeba histolytica*. *FEBS J.* 282, 318–331.
- [14] Bergmann, F. T., Hoops, S., Klahn, B., Kummer, U., Mendes, P., Pahle, J., Sahle, S. (2017) COPASI and its applications in biotechnology. *J. Biotechnol* 261, 215–220.
- [15] D'Alessandro, A., Kriebardis, A. G., Rinalducci, S., Antonelou, M. H., Hansen, K. C., Papassideri, I. S., Zolla, L. (2015) An update on red blood cell storage lesions, as gleaned through biochemistry and omics technologies. *Transfusion* 55, 205–219.
- [16] Rapoport, T. A., Heinrich, R., Rapoport, S. M. (1976) The regulatory principles of glycolysis in erythrocytes in vivo and in vitro. A minimal comprehensive model describing steady states, quasi-steady states and time-dependent processes. *Biochem. J.* 154, 449–469.
- [17] Holzhutter, H. G., Jacobasch, G., Bisdorff, A. (1985) Mathematical modeling of metabolic pathways affected by an enzyme deficiency. A mathematical model of glycolysis in normal and pyruvate-kinase-deficient red blood cells. *Eur. J. Biochem* 149, 101–111.
- [18] Yachie-Kinoshita, A., Nishino, T., Shimo, H., Suematsu, M., Tomita, M. (2010) A metabolic model of human erythrocytes: practical application of the E-Cell simulation environment. *J Biomed Biotechnol* 2010, 642420.
- [19] Kinoshita, A., Tsukada, K., Soga, T., Hishiki, T., Ueno, Y., Nakayama, Y., Tomita, M., Suematsu, M. (2007) Roles of hemoglobin allosterism in hypoxia-induced metabolic alterations in erythrocytes: Simulation and its verification by metabolome analysis. *J. Biol. Chem.* 282, 10731–10741.
- [20] van Wijk, R., van Solinge, W. W. (2005) The energy-less red blood cell is lost: Erythrocyte enzyme abnormalities of glycolysis. *Blood* 106, 4034–4042.
- [21] Kahir, T., Tacer, C. S., Ulgen, K. O. (2004) Metabolic pathway analysis of enzyme-deficient human red blood cells. *Biosystems* 78, 49–67.
- [22] Zancan, P., Sola-Penna, M. (2005) Regulation of human erythrocyte metabolism by insulin: Cellular distribution of 6-phosphofructo-1-kinase and its implication for red blood cell function. *Mol. Genet. Metab.* 86, 401–411.
- [23] Lewis, I. A., Campanella, M. E., Markley, J. L., Low, P. S. (2009) Role of band 3 in regulating metabolic flux of red blood cells. *Proc. Natl. Acad. Sci. U. S. A.* 106, 18515–18520.
- [24] Deng, D., Xu, C., Sun, P., Wu, J., Yan, C., Hu, M., Yan, N. (2014) Crystal structure of the human glucose transporter GLUT1. *Nature* 510, 121–125.
- [25] Dubinsky, W. P., Racker, E. (1978) The mechanism of lactate transport in human erythrocytes. *J. Membr. Biol.* 44, 25–36.
- [26] Halestrap, A. P. (2012) The monocarboxylate transporter family—Structure and functional characterization. *IUBMB Life* 64, 1–9.
- [27] Ferretti, A., Bozzi, A., Di Vito, M., Podo, F., Strom, R., Lewis, I. A., Campanella, M. E., Markley, J. L., Low, P. S. (1992) <sup>13</sup>C and <sup>31</sup>P NMR studies of glucose and 2-deoxyglucose metabolism in normal and enzyme-deficient human erythrocytes Role of band 3 in regulating metabolic flux of red blood cells. *Clin. Chim. Acta* 208, 39–61.





- [28] Aledo, J. C. (2001) Metabolic pathways: Does the actual Gibbs free-energy change affect the flux rate? *Biochem. Mol. Biol. Educ.* 29, 142–143.
- [29] Schmidt, M. M., Dringen, R. (2009) Differential effects of iodoacetamide and iodoacetate on glycolysis and glutathione metabolism of cultured astrocytes. *Front. Neuroenerg.* 1, 1.
- [30] Leal Denis, M. F., Alvarez, H. A., Lauri, N., Alvarez, C. L., Chara, O., Schwarzbaum, P. J. (2016) Dynamic regulation of cell volume and extracellular ATP of human erythrocytes. *PLoS ONE* 11, e0158305.
- [31] Christodouleas, D. C., Nemiroski, A., Kumar, A. A., Whitesides, G. M. (2015) Broadly available imaging devices enable high-quality low-cost photometry. *Anal. Chem.* 87, 9170–9178.
- [32] D'Alessandro, A., D'Amici, G. M., Vaglio, S., Zolla, L. (2012) Time-course investigation of SAGM-stored leukocyte-filtered red blood cell concentrates: From metabolism to proteomics. *Haematologica* 97, 107–115.
- [33] Kumagai, S., Narasaki, R., Hasumi, K. (2008) Glucose-dependent active ATP depletion by koningic acid kills high-glycolytic cells. *Biochem. Biophys. Res. Commun.* 365, 362–368.
- [34] Kato, M., Sakai, K., Endo, A. (1992) Koningic acid (heptelidic acid) inhibition of glyceraldehyde-3-phosphate dehydrogenases from various sources. *Biochim. Biophys. Acta* 1120, 113–116.
- [35] Endo, A., Hasumi, K., Sakai, K., Kanbe, T. (1985) Specific inhibition of glyceraldehyde-3-phosphate dehydrogenase by koningic acid (heptelidic acid). *J. Antibiot. (Tokyo)* 38, 920–925.
- [36] Bianchi, C., Genova, M. L., Parenti Castelli, G., Lenaz, G. (2004) The mitochondrial respiratory chain is partially organized in a supercomplex assembly: Kinetic evidence using flux control analysis. *J. Biol. Chem.* 279, 36562–36569.
- [37] Cortassa, S., O'Rourke, B., Winslow, R. L., Aon, M. A. (2009) Control and regulation of mitochondrial energetics in an integrated model of cardiomyocyte function. *Biophys. J.* 96, 2466–2478.
- [38] Cascante, M., Boros, L. G., Comin-Anduix, B., de Atauri, P., Centelles, J. J., Lee, P. W. (2002) Metabolic control analysis in drug discovery and disease. *Nat. Biotechnol.* 20, 243–249.
- [39] Boren, J., Montoya, A. R., de Atauri, P., Comin-Anduix, B., Cortes, A., Centelles, J. J., Frederiks, W. M., Van Noorden, C. J., Cascante, M. (2002) Metabolic control analysis aimed at the ribose synthesis pathways of tumor cells: A new strategy for antitumor drug development. *Mol. Biol. Rep.* 29, 7–12.
- [40] Gonzalez-Chavez, Z., Olin-Sandoval, V., Rodriguez-Zavala, J. S., Moreno-Sanchez, R., Saavedra, E. (2015) Metabolic control analysis of the Trypanosoma cruzi peroxide detoxification pathway identifies trypanodoxin as a suitable drug target. *Biochim. Biophys. Acta* 1850, 263–273.
- [41] Fell, D. A. (1998) Increasing the flux in metabolic pathways: A metabolic control analysis perspective. *Biotechnol. Bioeng.* 58, 121–124.
- [42] Cronwright, G. R., Rohwer, J. M., Prior, B. A. (2002) Metabolic control analysis of glycerol synthesis in *Saccharomyces cerevisiae*. *Appl. Environ. Microbiol.* 68, 4448–4456.
- [43] Acerenza, L., Ortega, F. (2007) Modular metabolic control analysis of large responses. *FEBS J.* 274, 188–201.
- [44] Ortega, F., Acerenza, L. (2002) Elasticity analysis and design for large metabolic responses produced by changes in enzyme activities. *Biochem. J.* 367, 41–48.